# Faster indentation influences skin deformation to reduce tactile discriminability of compliant objects

Bingxu Li, Student Member, IEEE, Steven C. Hauser, and Gregory J. Gerling, Senior Member, IEEE

Abstract—To discriminate the compliance of soft objects, we rely upon spatiotemporal cues in the mechanical deformation of the skin. However, we have few direct observations of skin deformation over time, in particular how its response differs with indentation velocities and depths, and thereby helps inform our perceptual judgments. To help fill this gap, we develop a 3D stereo imaging method to observe contact of the skin's surface with transparent, compliant stimuli. Experiments with humansubjects, in passive touch, are conducted with stimuli varying in compliance, indentation depth, velocity, and time duration. The results indicate that contact durations greater than 0.4 s are perceptually discriminable. Moreover, compliant pairs delivered at higher velocities are more difficult to discriminate because they induce smaller differences in deformation. In a detailed quantification of the skin's surface deformation, we find that several, independent cues aid perception. In particular, the rate of change of gross contact area best correlates with discriminability. across indentation velocities and compliances. However, cues associated with skin surface curvature and bulk force are also predictive, for stimuli more and less compliant than skin, respectively. These findings and detailed measurements seek to inform the design of haptic interfaces.

Index Terms—touch, tactile, softness, compliance, skin mechanics, stereo imaging, psychophysics.

#### I. INTRODUCTION

The skin is a deformable and stretchable organ embedded with thousands of neural afferents that encode mechanical contact interactions. Observations of its surface over time are vital to deciphering how we perceive the physical properties of objects, such as softness, roughness, and texture, amongst others. Within the broad category of softness [1], an object's compliance is important in our daily activities, e.g., inspecting the ripeness of fruit [2]. Understanding both how compliant stimuli are encoded at the skin's surface and how such deformation patterns evoke a percept is a fundamental topic and prerequisite in designing haptic actuators [3]–[5] and rendering algorithms [6].

Our percept of compliance is thought to be encoded, most notably, in cutaneous skin tissue near the contact interface [7]–[9], though also at joints and muscles [10], [11], non-contacting skin regions on the back of the digits and hand [12], and near the nail [13]. Moreover, as Xu, et al. show in modulating cutaneous inputs, our percept of compliance is a product of both sensation and volition [10]. At the skin contact interface, the relevant mechanical cues are not yet resolved, but likely involve gross contact area [7], [14], indentation depth [15], contact force [16], [17], skin stretch [15], [16], and surface stress [18].

<sup>1</sup>This work is supported in part by grants from the National Science Foundation (IIS-1908115) and National Institutes of Health (NINDS R01NS105241) to GJG. The funders had no role in study design, data collection and analysis, decision to publish, or preparation of the manuscript.

Also likely vital is their evolution over the time-course of contact [8], [19], [20].

To evaluate relationships of these mechanical cues with perception, a variety of empirical measurement techniques and experimental paradigms have been employed. For instance, in fabricating elastomeric slabs with controlled thickness and surface structure, Dhong et. al found that indentation depth and contact area contribute independently to perceived compliance [15]. Ink-based methods have estimated contact area at an indentation's terminal point [18], [20]. Similarly, stationary foam displays with a joint angle encoder have evaluated the contributions of finger displacement, joint angle, and change in contact area [7]. Spring cells with rigid plates have explored relationships of force and displacement, finding kinesthetic input alone is insufficient to discriminate compliance [21]. Similarly, Bergman Tiest and Kappers used elastomeric cylinders to compare kinesthetic force and displacement with cutaneous skin surface deformation cues, showing the importance of the latter [9], [22]. Moreover, sensors using piezoelectric materials at the skin surface have been built to assess contact area spread rate, pressure distribution, stress rate, slip detection, and force feedback [14], [23]–[25], while mechatronic devices have considered surface stretch [26], [27].

However, prior works have not directly observed the time-course of the skin surface while in contact with compliant objects, nor captured the how its deformation response differs with indentation velocity, depth, and duration, thereby shaping our perceptual judgments. These factors are necessary to consider because of the skin's non-linear and time-dependent properties [28]. Moreover, prior studies indicate indentation velocity can influence neural firing and our perception of compliance [29]–[31]. Therefore, in effort to tease apart the <sup>1</sup>mechanical cues at the skin surface that most optimally drive our perceptual response, across a range of stimuli varying in compliance, indentation depth, velocity, and time duration, the work herein develops equipment and an experimental approach to image the time-course of the skin surface while in contact with transparent, compliant stimuli.

## II. MATERIALS AND METHODS

To measure how spatiotemporal cues evolve over the course of contacting soft, compliant objects, we developed a 3D stereo imaging method. Silicone-elastomer stimuli were fabricated that span a range of compliances greater and lesser than that of the finger pad skin. From images of the skin surface taken through transparent stimuli, 3D point clouds that represent the geometry of the surface deformation of the finger pad are

The authors are with the School of Engineering and Applied Science, University of Virginia, Charlottesville, VA 22904, USA. The corresponding author is G. J. Gerling (phone: 434-924-0533; email: gg7h@virginia.edu).

generated every 100 ms using a disparity-mapping algorithm. These measurements were distilled into skin deformation cues of contact area, penetration depth, eccentricity, curvature, and force; and their time derivatives. Psychophysical experiments of pairwise discrimination, using a two-alternative forced-

choice (2AFC) strategy, in passive touch, were conducted across a prescribed range of stimulus compliances (5 to 184 kPa), as well as indentation depths (1.0 and 2.0 mm), velocities (1.0 to 6.5 mm/s), and time durations (0.3 to 2.0 s). In particular, the experimental paradigm included discrimination of stimuli

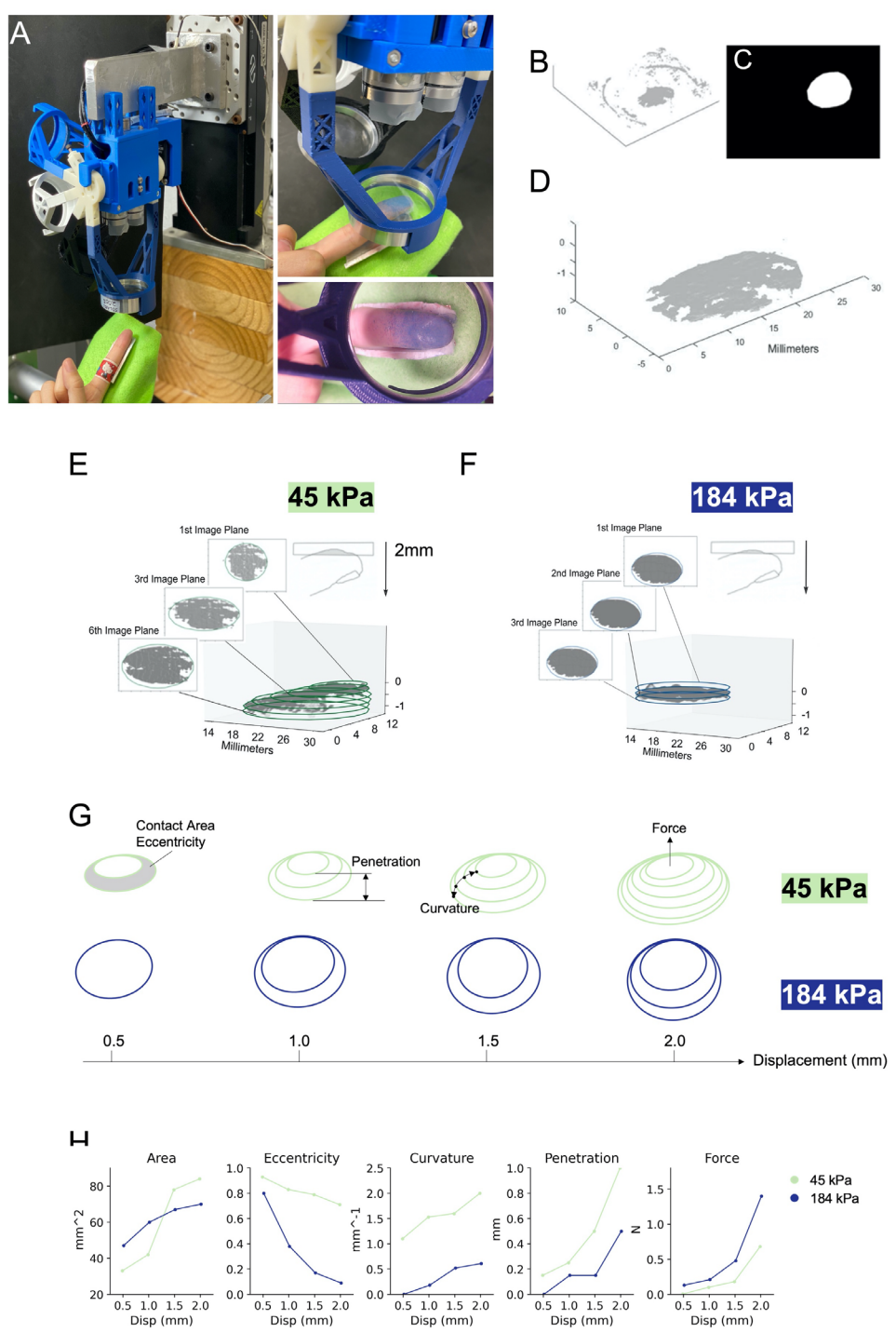


Fig. 1. Mechanical indentation and imaging apparatus, and data processing procedures, to capture 3D point clouds representing skin surface deformation upon indentation with compliant stimuli. (A) Apparatus with cantilever, 3D printed fixtures, cameras, load cell, and stimuli, relative to the indentation of a participant's finger. A 184 kPa stimulus in contact (left camera image) with a participant's finger pad at an indentation depth of 2 mm. (B-D) Data processing of a 3D point cloud, with raw data of the finger pad and partial outline of the aluminum ring at the surface image plane, masking of peripheral noise in the point cloud, and refined point cloud post-masking. (E-F) Ellipses are fit to each point cloud at image planes in 0.25 mm increments for more compliant (45 kPa) and less compliant (184 kPa) stimuli at a terminal indentation depth of 2 mm. (G) The evolution of the ellipses over the time course of a 2 mm indentation as the finger pad contacts stimuli of two compliances, along with a graphical description of the derived skin deformation cues. (H) The comparison of the time course evolution of five skin deformation cues between the two stimuli. One can observe, for instance, that the contact area is larger for the more compliant stimulus (45 kPa) and grows more slowly, while the force is higher for the less compliant stimulus (184 kPa).

less compliant than skin, more compliant than skin, and overlapping with the skin's compliance. As well, it includes three cases where the time duration was equalized by varying velocity and indentation depth (e.g., 2.5 mm/s at 1 mm and 4.5 mm/s at 2 mm, where both yield a time duration of 0.4 s).

#### A. Apparatus

An abbreviated description of the imaging apparatus is provided below and in Fig. 1A. For additional details on its validation, refer to prior work [32], [33]. Overall, the apparatus consists of an electrical-mechanical motion controller and load sled (ILS-100 MVTP, Newport, Irvine, CA, USA) with two cameras and a load cell installed on a cantilever. Up to five compliant stimuli can be delivered individually to a stationary finger pad at controlled indentation depth, velocity, and duration. Participants are seated in an adjustable chair with their elbow resting on a table surface during an experiment. Each participant's forearm is placed on a custom rigid support, oriented at an angle of 30 degrees with respect to the table's horizontal surface. A plastic curved support fixes the finger position beneath the point of contact.

An aluminum disk with a glass plate on the non-contact side houses each silicone-elastomer stimulus. Several stimuli were fabricated that vary in modulus and were mounted within custom 3D printed plastic arms to a rotary center, controlled by a servo motor. Displacement of a stimulus into the finger pad surface is controlled and measured by the motion controller, and force is measured at the stimulus by a load cell at 150 Hz, with a resolution of ±0.05 N (LCFD-5, Omegadyne, Sunbury, OH, USA). Two webcams (Papalook PA150, Shenzhen Aoni Electronic Industry Co., Guangdong, China) above the stimulus capture images at 30 frames per second, at a maximum resolution of 1280 by 720 pixels, and are able to maintain a manual focus.

## B. Compliant Stimuli Fabrication

Seven silicone-elastomer stimuli were constructed with modulus values from 5 to 184 kPa. For reference, the bulk modulus of human skin at the finger pad is about 42 - 54 kPa [34], [35]. One stimulus (45 kPa) lies within this range, with three stimuli fabricated to be more compliant (5, 10, 33 kPa) and three less compliant (75, 121, 184 kPa). Each formulation of silicone-elastomer was poured into its container, made by sealing a clean, dry glass disc (5.1 cm radius by 0.3 cm thick) into an aluminum collar (5.4 cm outer radius by 1.6 cm thick) using 0% diluted Solaris and heated at 100 Celsius until fully sealed. The more compliant stimuli (5, 10, 33 kPa) were made of two-component silicone rubber (Solaris, Smooth-on Inc., Macungie, PA, USA), mixed at a 1:1 ratio and then diluted with silicone oil (ALPA-OIL-50, Silicone oil V50, Modulor, Berlin, Germany) at ratios of 400% (4:1 ratios of silicone rubber to oil) for 5 kPa, 300% for 10 kPa and 200% for 33 kPa. Each stimulus rested at room temperature until its air bubbles were released, then cured in an oven at 100° Celsius for 25 min to fully solidify, before being returned to room temperature. To eliminate surface stickiness, a 0.04 mm layer of 100% diluted Solaris silicone rubber was applied to each substrate's surface, before being cured at 100° Celsius for 15 min. Stimuli harder than skin (75, 121, 184 kPa) were made of a different twocomponent silicone rubber (Sylgard 184, Dow Corning,

Midland, MI, USA), mixed with silicone oil at ratios of 100%, 50%, and 0% respectively. A sample (0.1 cm diameter by 0.1 cm height) was extracted for measuring the modulus of each stimulus formulation, indented by a glass plate at 1 mm/s velocity and 1 mm depth. The modulus of the stress-strain curve obtained from the force-displacement data was evaluated at 0.1 strain, following a standardized procedure [35].

## C. 3D Surface Reconstruction and Image Processing

To generate 3D point cloud data that captures the surface deformation of finger pad skin, a disparity-mapping based approach was used, as defined previously [32], [33]. Point clouds were obtained by co-locating the ink points on the skin surface. The identified pixel brightness values between left and right images are the coordinates of the points in the 3D domain (Fig 1B). For noise reduction, we first filtered out high-frequency noise caused by surrounding light sources, then manually extracted the area of contact between the skin and stimulus by masking the remaining areas (Fig 1C). On average, each 3D point cloud contains about 30,000 discrete points after noise reduction. We apply these two steps (filtering and masking) per image frame to ensure the data lie within the region of interest (Fig 1D).

## D. Ellipse Method to Generate Image Planes

To characterize the geometric change of the skin surface over the time-course of indentation, we developed a method to fit the 3D point cloud into vertically stacked ellipses with the same orientation [33]. The benefits of this ellipse representation are in its dimensionality reduction and data denoising, from 30,000 discrete points. We defined each ellipse as an image plane. Each ellipse contains at least 98% of the points in an image plane with 95% confidence. With the procedure, the 3D point cloud is divided into image planes at an increment of 0.25 mm, which is twice the resolution of the stereo images in the vertical dimension, i.e., 0.12 mm [32], starting from the plane representing surface contact through that with deepest finger pad penetration. Therefore, the first image plane was defined as the ellipse with deepest finger pad penetration and the last image plane represents the contact surface (Fig 1E, F).

## E. Derived Dependent Metrics

From using the ellipse method to characterize the geometric change of the skin surface, five dependent metrics, or skin deformation cues, were defined as penetration depth, curvature, eccentricity, contact area, and force.

Penetration depth is defined as the distance between the first and last image plane, in units mm, Eqn. 1, where N is number of image planes. Curvature is defined by discrete slope values averaged across all ellipses for that point cloud, Eqn. 2. The slope between two adjacent ellipses is estimated by the radius of the major axis of the ellipse and distance between them, with r as the radius and i the image plane.

$$P = (N - 1) * 0.25 \tag{1}$$

$$Slope_{ave} = \frac{\sum_{i=1}^{i=N} \frac{r(i+1) - r(i)}{r(i)}}{r(i)}$$
 (2)

$$e = \sqrt{1 - \frac{b^2}{a^2}} \tag{3}$$

Eccentricity is used to describe the shape of the contact surface, Eqn. 3, where a is the semi-major axis and b is the semi-minor axis of the defined ellipse. Eccentricity equals 0 if the contact shape is a perfect circle. Contact Area is the last image plane formed on the contact surface while Force is measured at the load cell. This method of estimating contact area has been validated previously [32], [36].

## F. Human Subjects Experimental Paradigm

Biomechanical measurements of skin surface deformation and psychophysical experiments of pairwise discrimination were conducted, in passive touch. The seven stimulus compliances (5, 10, 33, 45, 75, 121, and 184 kPa were delivered to the center of the finger pad individually, using displacement-control, at velocities of 1, 1.75, 2.5, 3.5, 4.5 and 6.5 mm/s to depths of both 1 and 2 mm, without any hold of the stimulus after the end of the ramp. The time duration of the loading phase ranged from 0.3 s (3.5 mm/s at 1 mm) to 2 s (1 mm/s at 2 mm).

## G. Participants

A total of 10 participants (mean = 23, SD = 1.2, 6 male and 4 female) were enrolled in the experiments, which all fully completed. The experiments were approved by the local Institutional Review Board, and informed consent was obtained from each participant. All devices and surfaces were sanitized after each use, and participants wore facemasks, according to SARS-COVID-2 protocols. During the perceptual experiments, participants were blindfolded to eliminate any visual cues.

## H. Psychophysical Experiments

A series of psychophysical experiments of pairwise discrimination were performed to evaluate combinations of stimulus compliance, across indentation velocity, depth and duration. Four compliant pairs (184/121, 33/5, 45/10, and 45/75 kPa) were used, whereby the 184/121 kPa pair is less compliant than the skin, and the 33/5 kPa is more compliant than the skin, and the remaining pairs span the skin's modulus in either direction. Each stimulus of a pair of stimuli was delivered to a participant's finger pad sequentially in randomized order with a 2 s interval. Participants reported which of the two stimuli was more compliant, either first or second. In total, there were 4.800 indentations, consisting of 2 stimuli within a pair, 4 compliant pairs, 6 velocities, 2 depths, 5 repetitions, and 10 participants. The average experimental duration per participant was about 80 min including breaks. The biomechanical and psychophysical experiments could have been conducted all in one, but we separated them to attain the highest quality imaging data. Such can involve cleaning a small amount of residue from the transparent stimuli, which requires time per indentation (3-5 s) and can produce a lengthier, inconsistent duration between paired psychophysical experiments. Furthermore, each participant's psychophysical experiment was conducted before their biomechanical experiment, as it required greater cognitive attention.

## I. Biomechanical Experiments

A series of biomechanical experiments of skin surface deformation evaluated these same stimulus combinations. In total, we analyzed 2,520 indentations, including 7 stimulus compliances, 6 velocities, 2 depths, 3 repetitions, and 10 participants. Note that at the indentation depth of 1 mm, since the compliant pairs were not discriminable at 3.5 mm/s, we did not examine velocities any faster. The average time to complete this experiment was 70 min, including a 10 min break. At the beginning of each participant's experiment, their index finger was secured to a curved plastic support and a thin layer of blue ink was applied using a paint brush, with its bristles normal to the skin surface. Each stimulus was brought into the finger pad with a light contact force (< 0.1 N) before indentation, then slowly retracted to 0 N. This pre-calibration procedure helped ensure a consistent contact state between trials.

#### J. Statistical Analysis

All image processing procedures were performed using MATLAB Computer Vision Toolbox and all data analysis were performed using Python 3.6. ANOVA tests evaluated statistical differences at p < 0.05.

#### III. RESULTS

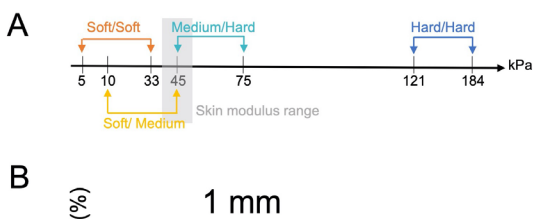
## A. Results of Psychophysical Experiments

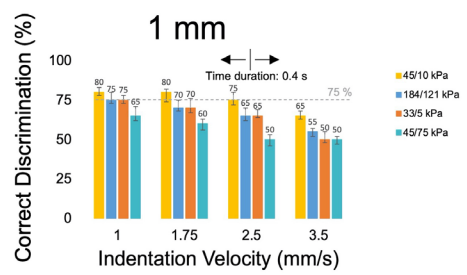
Fig 2A illustrates the modulus of the four compliant pairs, relative to the bulk modulus of the skin. Figs. 2B-C show the results in discriminating stimuli at 1 and 2 mm indentation depths, across indentation velocities. Overall, no participant was able to discriminate a stimulus pair at a time duration of less than 0.4 s. In particular, the 45/10 kPa compliant pair was discriminable above 75% correct at indentation velocities of 2.5 and 4.5 mm/s, and slower, at depths of 1 and 2 mm, respectively. Moreover, as Figs. 2B-C indicate, participants were less able to correctly discriminate compliant pairs at lower displacements and higher velocities. The 45/10 kPa pair was the most discriminable, and nearly so at a velocity of 6.5 mm/s at 2 mm. In contrast, the 75/45 kPa compliance pair was never reached a 75% level of correct discrimination. The discrimination rates for the 184/121 and 33/5 kPa pairs were higher than the 75% discrimination threshold, where the compliance values of these pairs lie to either side of the skin's modulus.

Furthermore, we performed a 3-way repeated ANOVA test of the major experimental factors, yielding significant effects for compliant pair ( $F_{3,387} = 565.7$ , p < 0.001), velocity ( $F_{5,387} = 1427.8$ , p < 0.0001) and depth ( $F_{1,387} = 1072.5$ , p < 0.0001).

## B. Approach 1: Skin Deformation at Discrete Time Points

In a first approach to comparing the skin deformation cues and perceptual judgments, we evaluated the cues at discrete observation time points, every 0.1 s. In particular, we conducted pairwise statistical t-tests between compliant pairs every 0.1 s from 0.1 s to the terminal duration of that indentation. Data for the eccentricity cue are shown in Fig. 3, with that for all cues in Appendix, Figs. 1 and 2. As can be observed in Fig. 3A, at a stimulus depth of 1 mm and velocity of 1.75 mm/s, there are 6 observation points for each of the 7 compliant stimuli, where eccentricity decreases with indentation time. In Fig. 3B, the 0.6





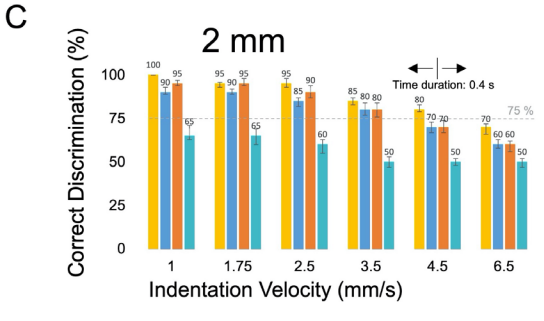


Fig. 2. Psychophysical evaluation of compliant pairs across indentation depths and velocities. The error bar represents two standard deviations within the sample. In panel (A), four compliant pairs were selected to be more compliant than that of the skin (33/5 kPa), less compliant than skin (184/121 kPa) and overlapping (75/45 and 45/10 kPa). Skin stiffness is about 42 – 54 kPa. (B) Pairwise perceptual evaluation of stimuli indented sequentially into the passive index finger pad to 1 mm depth at four indentation velocities, resulting in time durations of 1, 0.56, 0.4, 0.3 s. (C) Stimulus indentation to 2 mm depth at six indentation velocities, resulting in time durations of 2, 1.14, 0.8, 0.56, 0.4, 0.3 s. The findings indicate that the compliant pairs are not discriminable before a time duration of 0.4 s. Beyond that time point, pairs delivered at higher velocities are more difficult to discriminate. The 45/10 kPa pair is the most discriminable and the 75/45 kPa pair is not discriminable above a level 75% for any indentation velocity.

s time point alone is analyzed, as highlighted with the grey bar in Fig. 3A. Statistical evaluations of four compliant pairs are given in Fig. 3C, where a colored tile indicates statistical significance (p<0.05), and the framework's background of white (1 mm depths) or grey (2 mm depths) indicates a lack of statistical significance. These four pairs are all statistically significant. Note in Fig. 3C the red frames around a group of four tiles, which refers to an evaluation of perceptual discriminability at or above 75% correct, with a diagonal within these tiles indicating a lack of perceptual discriminability. These data come from Fig. 2. In this way, one can compare differences in skin deformation cues and perceptual judgments.

At least two observations can be made in Fig. 3. First, for some of the cues, notably eccentricity, we observe statistical differences in the skin deformation between compliant pairs before they are perceptually discriminable. For example, at a depth of 1 mm and velocity of 1.75 mm/s, the eccentricity cue is distinct for all four compliant pairs at 0.6 s, even though only the 45/10 kPa pair is perceptually discriminable, Fig. 3C. Second, we observe the force cue is distinct only for the less compliant 184/121 kPa pair, Fig. 3D, whereas the perceptual predictiveness of the contact area cue is mixed, Fig. 3E.

Indeed, with this approach we observe differences in skin deformation at early time durations, before they are perceptually discriminable. However, several issues arise in using this approach to tie the skin deformation cues with the perceptual outcomes. In particular, it cannot differentiate if perceptual differences are informed by the skin cues at that given observation's time point or accumulated over multiple prior time points. If only individual time points are evaluated, then no time history information is included, yet Fig. 2 indicates that time duration and velocity impact perception. For this reason, we sought a second approach to evaluate how the cues evolve over time, in line with prior works [37]–[39].

## C. Approach 2: Change Rates of Skin Deformation over the Time Course of the Indentation

In a second approach to comparing the skin deformation cues and perceptual judgments, we evaluated change rates in the cues, per indentation, over the time course of the indentation. In this way, the single estimate produced per indentation is made, and then compared with that of the other stimulus of the pair.

An example application of this procedure is given in Fig. 4. Fig. 4A-B describes forming a singular estimate of the magnitude for a first stimulus, then an estimate of a second stimulus, so to difference those estimates to generate a single discriminability estimate, Fig. 4C. In particular, the change rates of contact area for 45 and 10 kPa stimuli at 1.75 mm/s velocity are calculated as 48 mm<sup>2</sup>/s and 67 mm<sup>2</sup>/s, Fig. 4A. Over the series of change rates representing the entire time course of an indentation, the middle value in the sequence is selected. The median value was used, rather than the mean, to better represent the central tendency over the indentation and be robust to outliers given the distribution of our datasets. Next, in Fig. 4B, these median change rates at the 1.75 mm/s velocity, and at all velocities, are plotted. Building up further, Fig. 4C shows the contact area rate difference from Fig. 4B for this 45/10 kPa compliant pair, and all compliant pairs across all velocities. The results in Fig. 4C indicate that the contact area rate difference decreases as velocity increases, especially for the 45/10 kPa compliant pair. Also the order of the stimulus pairs in Fig. 4C, with 45/10 kPa first, then 35/5 and 184/121 kPa, and 75/45 kPa follows discrimination results in Fig. 2.

In effort to statistically correlate the skin deformation cues with the perceptual judgments, we performed a regression analysis. A subset of the perceptual results for two indentation velocities are plotted in Fig. 4D, with contact area rate differences in Fig. 4E. Then regression is performed between these two variables, Figs. 4F-G. The analysis for the entire set of velocities and depths can be found in the Appendix, Fig 4. The results indicate that the contact area cue well correlates with perceptual discrimination across the compliant pairs and indentation velocities, with  $R^2$  values greater than 0.7. Correlations for cues of contact area, as well as curvature, force and eccentricity, are summarized in Fig. 4H. Interestingly, the curvature cue exhibits high correlation with the perceptual results for the more compliant pairs (33/5 and 45/10 kPa). In contrast, the force cue exhibits high correlation for the less compliant pairs (184/121 and 75/45 kPa), while the eccentricity cue is well correlated at the extremes of the compliant pairs away from the stiffness of the skin (184/121 and 33/5 kPa pairs). The rate difference data that underlies these cues can be

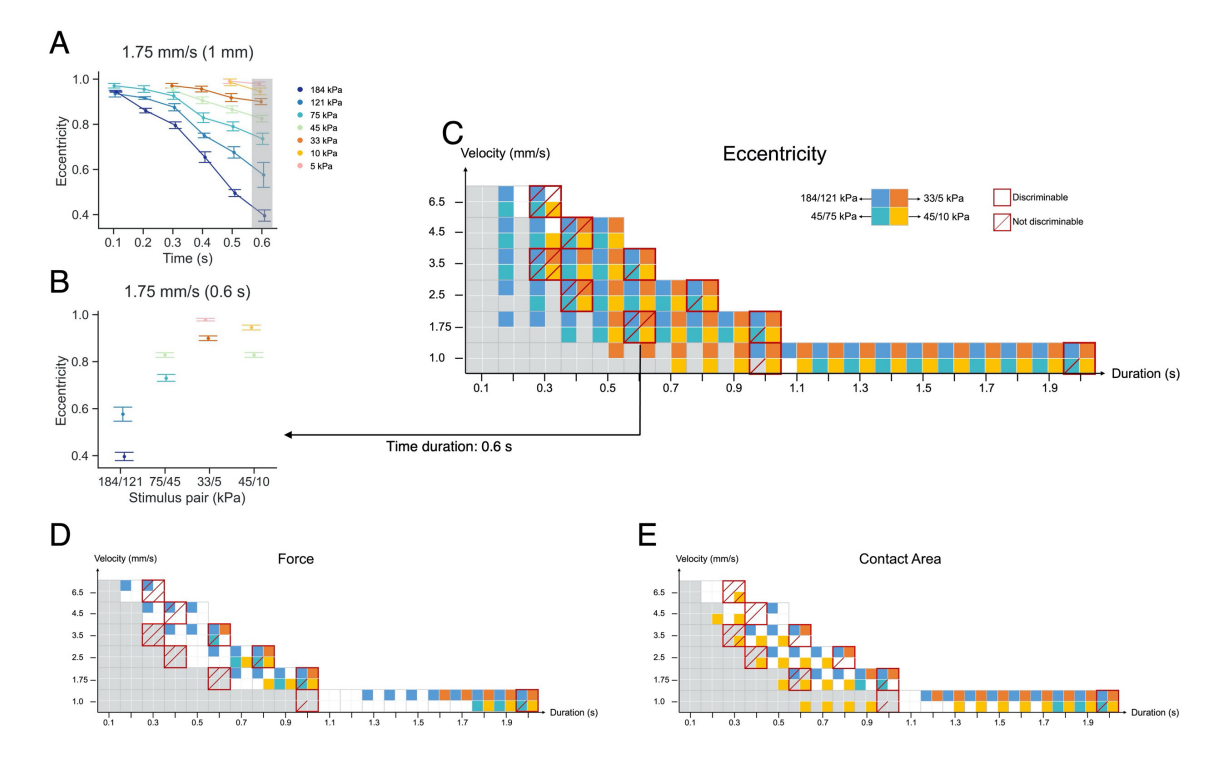


Fig. 3. Using Approach 1 to compare skin deformation cues calculated at discrete time points with the perceptual results, across the compliant pairs, indentation velocities and displacements. As a unit, panels (A-C) describe the approach 1 process for the eccentricity cue. (A) Observations for eccentricity over the time course of indentation for the seven stimulus compliances at a velocity of 1.75 mm/s and displacement of 1 mm. The error bar indicates two standard deviations. (B) The four compliant pairs at 0.6 s from panel (A). (C) An evaluation of statistical significance for these four compliant pairs, where each block represents an evaluation of a compliant pair, and the use of colored block, as opposed to the gray or white framework, indicates statistical significance for this condition. Blocks in the framework with a grey background represent a stimulus displacement of 1 mm and a white background 2 mm. Moreover, blocks outlined in red indicate compliant pairs where psychophysical experiments were conducted, with open blocks being perceptually discriminable above 75% and a crossed-out blocks represent a lack of discriminability at that level. These data come from Fig. 2. For the eccentricity cue, the blocks in (C) indicate that all four compliant pairs are statistically different, yet only the 45/10 kPa pair is perceptually discriminable. Panel (D) shows the results for force cue which is more distinct for the less compliant pairs, and (E) shows the results for contact area cue which indicates mixed results. In summary, Approach 1 does not lead to clear connections between any of the cues and the perceptual outcomes.

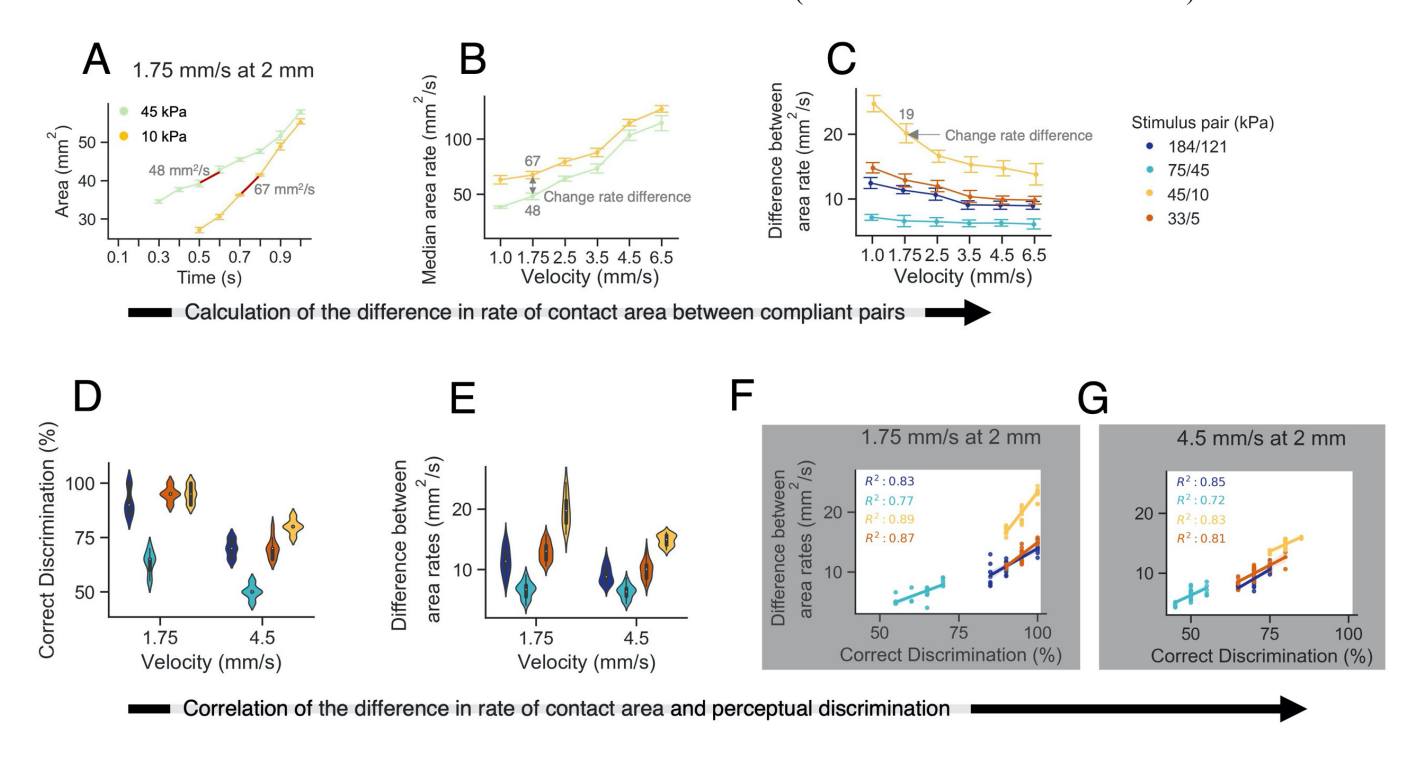
found in Appendix, Fig. 3. Indeed, it indicates that the difference in the curvature change rates decreases with velocity only for the more complaint pairs (33/5 and 45/10 kPa); the difference in force rates decreases for the less compliant pairs (184/121 and 75/45 kPa); and decreases for eccentricity for all except the 45/10 kPa pair.

Moreover, as associated with the results in Fig. 4H, we conducted a one-way ANOVA to evaluate the dependency of overall rate difference in skin deformation cues on discrimination performance per compliance pair, across all velocities. The results indicate that perceptual discrimination is significantly associated with differences for contact area for all compliant pairs ( $F_{1,175} = 19.6$ , p < 0.05 for 184/121 kPa pair,  $F_{1,175} = 22.1, p < 0.01$  for 75/45 kPa pair,  $F_{1,174} = 88.8, p < 0.001$ for 45/10 kPa pair,  $F_{1.174} = 27.2$ , p < 0.01 for 33/5 kPa pair), whereas curvature is correlated with discrimination only for  $45/10 \text{ kPa} (F_{1,174} = 30.1, p < 0.001) \text{ and } 33/5 \text{ kPa} (F_{1,174} = 16.3, p < 0.001)$ p < 0.05) pairs, compared to the force cue, which is only significant for the less compliant pairs ( $F_{1,175} = 25.8$ , p < 0.01for 184/121 kPa pair,  $F_{1,175} = 26.3$ , p < 0.01 for 75/45 kPa pair), and the eccentricity cue has an impact on perception for 184/121 kPa ( $F_{1,175}$  = 49.0, p < 0.001), 75/45 kPa ( $F_{1,175}$ = 31.2, p < 0.001), and 33/5 kPa ( $F_{1,174} = 20.9$ , p < 0.05) compliant

In summary, correlations between skin surface deformation and perceptual judgements are observed across the stimulus compliance and indentation velocity. However, the highest correlations are observed between rate differences in contact area, which are consistent across all compliances and velocities. Moreover, curvature exhibits high correlation for the more compliant stimuli, force for the less compliant stimuli, and eccentricity for the most and least compliant stimulus pairs. The utility of the force cues with less compliant stimuli, in particular, align with prior psychophysical studies which have utilized stiffer stimuli [2], [10], [20], [40], [41]. The eccentricity cue, which describes the contact shape, has been found to be correlated with percept of friction [42]. The work herein supplements such with results with more information on the utilization of cues for predicting perception regarding factors of stimulus compliance, indentation velocity and depth.

#### D. Dependency between Skin Deformation Cues

As indicated in Fig. 4H, the perceptual results may be associated with more than a single cue, e.g., for the less compliant 184/121 kPa pair, where both contact area and force are strong predictors. Therefore, we evaluated the degree of independence between the cues in statistical correlations conducted across stimulus compliance, indentation velocity and depth, using Pearson correlation. Of all the cues in Fig 5, only one, penetration depth, relatively highly correlates with other cues, in particular curvature (r = 0.70, p < 0.001) and contact area (r = 0.62, p < 0.001), in agreement with prior works [20].



Н						
	Cues (R <sup>2</sup> ) (kPa)	Area	Curvature	Force	Eccentricity	
	184/121	0.83	0.32	0.91	0.75	- 1.75 mm/s at 2 mm
		0.85	0.42	0.82	0.70	- 4.5 mm/s at 2 mm
	75/45	0.77	0.46	0.75	0.66	-
	75/45	0.72	0.53	0.71	0.59	
	45/10	0.89	0.76	0.37	0.52	_
		0.83	0.72	0.50	0.58	_
	33/5	0.87	0.89	0.22	0.74	-
		0.81	0.88	0.43	0.71	-

Fig. 4. Using Approach 2 to compare the difference in rate of change in contact area between compliant pairs with discrimination performance. (A-B) An example of the steps in calculating the rate differences in contact area, from discrete time points to change rate across six velocities. Change rates of contact area for 45 and 10 kPa stimuli at 1.75 mm/s velocity are calculated, with median values of 48 mm²/s and 67 mm²/s. Change rates at all velocities are plotted. (C) The contact area rate difference for the 45/10 kPa compliant pair, as well as all compliant pairs across all velocities, showing a decrease with increased indentation velocity. The error bar is computed using bootstrapping, showing estimates of the true mean and 95% confidence. (D) Psychophysical discrimination results from Fig. 2 for the four compliant pairs at 1.75 and 4.5 mm/s velocities in which there are 50 points per compliant pair per velocity, and (E) corresponding differences in contact area rate differences from (C). (F-G) Regression associates contact area rate difference with discrimination per compliance pair, with correlations listed. (H) Summary of the correlations of all skin deformation cues, with those higher than 0.7 are highlighted in gray. In summary, high correlations between rate differences in contact area are observed across all compliances and velocities, while curvature exhibits high correlation for the more compliant stimuli, force for the less compliant stimuli, and eccentricity for the most and least compliant stimulus pairs.

The low degree of correlation between the other cues implies statistical independence, indicating together with Fig. 4 that we indeed may utilize more than just one skin deformation cue to form perceptual judgments.

#### IV. DISCUSSION

As we go about daily interactions with soft and compliant objects, the neural afferents innervating our skin signal patterns in its surface deformation. Such patterns are shaped by the compliance of a contacting object relative to the skin's stiffness, as well as its indentation velocity, depth, and duration. This work sought to better understand both how compliant stimuli

are encoded in patterns of deformation at the skin's surface and how such patterns may be correlated with evoked percepts. These are fundamental topics in somatosensory perception and prerequisites in designing haptic actuators and rendering algorithms.

Herein, we conducted human-subjects experiments with a custom-built 3D stereo imaging system to observe the skin through transparent, compliant stimuli. The results show that a minimum contact duration of at least 0.4 s is required for perceptual discriminability. Beyond that point, compliant pairs delivered at higher velocities are increasingly difficult to discriminate, in agreement with smaller changes in skin

deformation. In a detailed quantification of the skin's surface deformation, we find that several, independent cues aid in the discrimination of compliant pairs. In particular, we find that temporal changes in the gross contact area well correlate with discriminability, regardless of stimulus compliance and indentation velocity. However, other independent cues tied to surface curvature, eccentricity, and bulk force are likely complementary in informing perceptual judgements, in certain situations, e.g., bulk force when a contacting object is less compliant than the skin itself.

#### A. Indentation duration and velocity shape discrimination

We find that a contact duration of 0.4 s is required for perceptual discriminability. This observation is robust across combinations of indentation depths and velocities, which vary the stimulus duration between 0.3 - 2.0 s, Fig. 1B-C. In particular, the 45/10 kPa pair is discriminable in two cases where time duration is 0.4 s, both a velocity of 2.5 mm/s and indentation depth of 1 mm, and at 4.5 mm/s and 2 mm, indicating that the duration of the indentation is impactful beyond its velocity alone. At constant depths of indentation, slower velocity results in longer duration contact, which has been shown to facilitate a greater accumulation of information [38], [39]. With a shorter duration of contact, the relatively weaker contribution of the first stimulus makes it more difficult to discriminate from the second stimulus. Interestingly, in terms of observations of skin deformation, in particular contact area, we begin to observe pairwise differences between the 45/10 kPa stimulus pair slightly earlier, at 0.3 s.

The study's experimental paradigm also varied the velocity of the indentation ramp from 1 - 6.5 mm/s to evaluate its effects on skin deformation and perception. We observe a greater degree of perceptual discriminability between compliant pairs at the slower velocities, Fig. 2B-C. Discriminability was reliable across three compliant pairs at 1 mm/s for the 1 mm depth and 3.5 mm/s for the 2 mm depth. Likewise, we observed greater differences in the skin's deformation between compliant pairs at slower velocities, in particular, for the contact area rate cue, Fig. 4C, but also for the curvature, eccentricity and force rate cues (Appendix, Fig. 2). Moreover, at velocities of 1.75 mm/s and 4.5 mm/s, the skin deformation cues, in particular the change rate of contact area between compliant pairs are well correlated with rates of perceptual discrimination, Fig. 4H. Indeed, prior studies have indicated that indentation velocity can influence neural firing and our perception of compliance [29]–[31]. For instance, LaMotte and Srinivasan found the discharge rate of neural afferents increases monotonically with velocity. As denoted by our findings herein, we extend these efforts by defining the contributions of those skin deformation cues that are most robust at reliably encoding object compliances across a range of indentation velocities.

#### B. The utility of distinct skin deformation cues

In a detailed quantification of the skin's surface deformation, we find that several cues independently aid in the discrimination of compliant pairs. Among the five skin deformation cues, the change rate of contact area over the indentation is most highly correlated with perceptual judgments. In particular, large differences in this cue between compliant pairs were observed across the full range of object

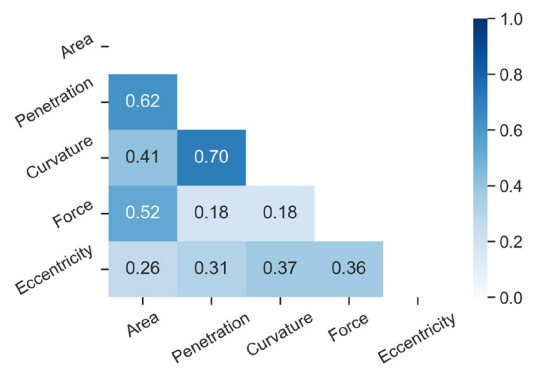


Fig 5. Evaluating the degree of independence between the skin deformation cues (change rates from Approach 2). Only the penetration depth cue exhibits a relatively high correlation with curvature (r = 0.70, p < 0.001) and contact area (r = 0.62, p < 0.001). The low degree of correlation between the rest of cues implies they are not statistically dependent on each other.

compliances, which well correlate with rates of perceptual discrimination ( $R^2$  values of 0.72 to 0.89), Fig. 4H. That said, other cues related to skin surface curvature and bulk force were correlated with perceptual judgments, for stimuli more and less compliant relative to the skin, respectively, Fig. 4H. In this way, the findings indicate that the change rate of contact area is a very useful all-around cue, though not per se at static or terminal snapshots in time. Compared to prior work which has pointed to the utility of contact area cues [7], [14], [15], [23], we distinguish its rate of change. Encoding via a rate of change metric also appears to be important in accounting for individual differences in skin properties [14], [19], [23], and in active touch, where volitional movements are made to optimize force rate while minimizing object deformation [10], [20].

The magnitudes of contact area measured in this study align closely with prior efforts using both rigid [43]-[45] and elastic [7], [20], [32], [34] stimuli in passive touch. In particular, using an ink-based technique, Hauser and Gerling measured the contact area as about 80 and 65 mm<sup>2</sup> when the finger pad was indented by 120 and 22 kPa stimuli at a 2 mm depth, respectively. Similarly, the measurements in this study range from 78 mm<sup>2</sup> for 121 kPa and 54 mm<sup>2</sup> for 10 kPa stimuli. Similarly, Dzidek et al. estimated contact areas of about 90 and 100 mm<sup>2</sup> at forces of 1 and 1.5 N, when the finger was indented by a rigid plate at a 30-degree angle, which is close to our measurements of 83, 89 mm<sup>2</sup> for the 184 kPa stimulus that has a lower modulus than a rigid plate [43]. That stated, one should note that magnitudes of contact area measured in the literature can vary significantly to the differences in experimental setup, such as finger contact angle and stimulus geometry.

In addition to contact area, other skin deformation cues appear to be fruitful dependent on object compliance relative to the skin. Herein we evaluated the discriminability of four compliant pairs (184/121, 33/5, 45/10, and 45/75 kPa), whereby the 184/121 kPa pair was less compliant than skin, and 33/5 kPa was more compliant than skin, and the remaining pairs spanned the skin's modulus in either direction. The results indicate unique patterns in skin deformation. For example, in Fig. 4, with the highly compliant 45/10 kPa pair, we observed the best correlation with perceptual judgments for contact area and curvature, whereas for the less compliant 184/121 kPa pair, contact area and force produce the highest correlation. These

findings also hold when the cues are evaluated at discrete time points using Approach 1, Fig. 3. In comparison with prior literature, our measurement of force is about 0.75 N at 1 mm/s velocity for a soft stimulus (45 kPa), similar with 0.7 N at 0.5 mm/s for compliant stimuli [21], [41], and our results also align with the perceptual utility of the force cue for less compliant stimuli [2], [10], [20], [40], [41]. Indeed, most prior studies use stiff stimuli, relative to skin [35], and for this reason may be distorting our understanding of a broader range of compliant interactions. Furthermore, we note that the compliant pairs at equal 30 kPa intervals, i.e., 33/5 and 75/45 kPa, exhibit different rates of discriminability and preferred skin deformation cues. This distinction indicates a sensitivity to objects more compliant than the skin that is perhaps ecologically driven. Although further work is necessary to fully define the nonlinearities in touch relative to stimulus modulus, such perceptual tuning aligns with psychophysical findings in audition.

## C. Discrimination strategies for rate-based encoding

Two approaches were developed to compare skin deformation cues and perceptual judgments. In particular, with our imaging setup, we evaluated skin deformation cues at discrete observation time points (Approach 1) as well as by their change rates over the indentation (Approach 2). We found that cues associated with the latter approach better correlated with discriminability. Over the series of change rates representing the entire time course of an indentation, our approach used the middle value in the sequence. This was done, rather than using the mean, to represent the central tendency of the data over the indentation and to be robust to outliers. Other approaches could have averaged or summed the data or accumulated change rates in a temporally weighted manner.

Others have employed somewhat similar approaches. For example, Xu et.al (2020) evaluated the dissimilarity between force rates based on the discrete time differences in discriminating between naturalistic objects, and found a correlation with perceptual performance [37]. Indeed, memory representations in discriminating compliance are affected by exploration length and temporal delay in which haptic information is gathered and integrated in a continuous manner [38], [39]. Further efforts, likewise, have shown that temporalbased cues such as accumulative discrete-time difference and average change rate difference, are largely correlated with perceptual discrimination [9], [19], [20], [23], [33], as opposed to cues defined at terminal indentation [7], [14], [15]. Additional efforts will be required to refine the nature of how information is accumulated over time in order to arrive at judgments.

#### ACKNOWLEDGMENTS

We would like to thank all the participants of the humansubjects experiments, as well as members of the Gerling Touch Lab for fruitful discussions and feedback. This work was supported in part by grants from the National Science Foundation (IIS-1908115) and National Institutes of Health (NINDS R01NS105241). The content is solely the responsibility of the authors and does not necessarily represent the official views of the NSF or NIH.

#### REFERENCES

- [1] M. Cavdan, K. Doerschner, and K. Drewing, "Task and material properties interactively affect softness explorations along different dimensions," *IEEE Trans. Haptics*, pp. 1–1, 2021, doi: 10.1109/TOH.2021.3069626.
- [2] C. Xu, H. He, S. C. Hauser, and G. J. Gerling, "Tactile Exploration Strategies With Natural Compliant Objects Elicit Virtual Stiffness Cues," *IEEE Trans. Haptics*, vol. 13, no. 1, pp. 4–10, Jan. 2020, doi: 10.1109/TOH.2019.2959767.
- [3] G. Frediani, H. Boys, M. Ghilardi, S. Poslad, J. J. C. Busfield, and F. Carpi, "A Soft Touch: Wearable Tactile Display of Softness Made of Electroactive Elastomers," *Adv. Mater. Technol.*, vol. n/a, no. n/a, p. 2100016, doi: https://doi.org/10.1002/admt.202100016.
- [4] S. Mun *et al.*, "Electro-Active Polymer Based Soft Tactile Interface for Wearable Devices," *IEEE Trans. Haptics*, vol. 11, no. 1, pp. 15–21, Jan. 2018, doi: 10.1109/TOH.2018.2805901.
- [5] I. Poupyrev and S. Maruyama, "Tactile interfaces for small touch screens," in *Proceedings of the 16th annual ACM* symposium on *User interface software and technology*, New York, NY, USA, Nov. 2003, pp. 217–220. doi: 10.1145/964696.964721.
- [6] M. C. Lin and M. A. Otaduy, *Haptic rendering: Foundations, algorithms, and applications.* 2008.
- [7] A. Moscatelli *et al.*, "The Change in Fingertip Contact Area as a Novel Proprioceptive Cue," *Curr. Biol.*, vol. 26, no. 9, pp. 1159–1163, May 2016, doi: 10.1016/j.cub.2016.02.052.
- [8] M. A. Srinivasan and R. H. LaMotte, "Tactual discrimination of softness: abilities and mechanisms," in *Somesthesis and the Neurobiology of the Somatosensory Cortex*, P. O. Franzén, P. R. Johansson, and P. L. Terenius, Eds. Birkhäuser Basel, 1996, pp. 123–135. doi: 10.1007/978-3-0348-9016-8 11.
- [9] W. M. Bergmann Tiest and A. M. Kappers, "Cues for haptic perception of compliance," *Haptics IEEE Trans. On*, vol. 2, no. 4, Art. no. 4, 2009.
- [10] C. Xu, Y. Wang, and G. J. Gerling, "An elasticity-curvature illusion decouples cutaneous and proprioceptive cues in active exploration of soft objects," *PLOS Comput. Biol.*, vol. 17, no. 3, p. e1008848, Mar. 2021, doi: 10.1371/journal.pcbi.1008848.
- [11] K. Johnson, "Closing in on the neural mechanisms of finger joint angle sense. Focus on 'Quantitative analysis of dynamic strain sensitivity in human skin mechanoreceptors," J. Neurophysiol., vol. 92, no. 6, pp. 3167–3168, Dec. 2004.
- [12] B. B. Édin, "lamotte\_softness\_2000," *J. Neurophysiol.*, vol. 67, no. 5, pp. 1105–1113, May 1992, doi: 10.1152/jn.1992.67.5.1105.
- [13] I. Birznieks, V. G. Macefield, G. Westling, and R. S. Johansson, "Slowly Adapting Mechanoreceptors in the Borders of the Human Fingernail Encode Fingertip Forces," *J. Neurosci.*, vol. 29, no. 29, pp. 9370–9379, Jul. 2009, doi: 10.1523/JNEUROSCI.0143-09.2009.
- [14] G. Ambrosi, A. Bicchi, D. De Rossi, and E. P. Scilingo, "The role of contact area spread rate in haptic discrimination of softness," in *Proceedings 1999 IEEE International Conference on Robotics and Automation (Cat. No.99CH36288C)*, May 1999, vol. 1, pp. 305–310 vol.1. doi: 10.1109/ROBOT.1999.769996.
- [15] C. Dhong et al., "Role of indentation depth and contact area on human perception of softness for haptic interfaces," Sci. Adv., vol. 5, no. 8, p. eaaw8845, Aug. 2019, doi: 10.1126/sciadv.aaw8845.
- [16] M. Liu, A. Batista, S. Bensmaia, and D. J. Weber, "Information about contact force and surface texture is mixed in the firing rates of cutaneous afferent neurons," *J. Neurophysiol.*, vol. 125, no. 2, pp. 496–508, Feb. 2021, doi: 10.1152/jn.00725.2019.

- [17] M. Di Luca, B. Knörlein, M. O. Ernst, and M. Harders, "Effects of visual-haptic asynchronies and loading-unloading movements on compliance perception," *Brain Res. Bull.*, vol. 85, no. 5, pp. 245–259, Jun. 2011, doi: 10.1016/j.brainresbull.2010.02.009.
- [18] C. Schuermann, R. Haschke, and H. Ritter, "Modular high speed tactile sensor system with video interface," Jan. 2009.
- [19] B. Li and G. J. Gerling, "Individual differences impacting skin deformation and tactile discrimination with compliant elastic surfaces," in 2021 IEEE World Haptics Conference (WHC), Jul. 2021, pp. 721–726. doi: 10.1109/WHC49131.2021.9517222.
- [20] S. C. Hauser and G. J. Gerling, "Force-rate Cues Reduce Object Deformation Necessary to Discriminate Compliances Harder than the Skin," *IEEE Trans. Haptics*, vol. 11, no. 2, pp. 232– 240, Apr. 2018, doi: 10.1109/TOH.2017.2715845.
- [21] M. A. Srinivasan and R. H. LaMotte, "Tactual discrimination of softness," *J. Neurophysiol.*, vol. 73, no. 1, Art. no. 1, 1995.
- [22] W. M. Bergmann Tiest and A. M. Kappers, "Physical Aspects of Softness Perception," in *Multisensory Softness*, Springer London, 2014, pp. 3–15. Accessed: Jan. 19, 2017. [Online]. Available: http://link.springer.com/chapter/10.1007/978-1-4471-6533-0
- [23] A. Bicchi, E. P. Scilingo, and D. De Rossi, "Haptic discrimination of softness in teleoperation: the role of the contact area spread rate," *IEEE Trans. Robot. Autom.*, vol. 16, no. 5, pp. 496–504, Oct. 2000, doi: 10.1109/70.880800.
- [24] W. Chen, H. Khamis, I. Birznieks, N. F. Lepora, and S. J. Redmond, "Tactile Sensors for Friction Estimation and Incipient Slip Detection—Toward Dexterous Robotic Manipulation: A Review," *IEEE Sens. J.*, vol. 18, no. 22, pp. 9049–9064, Nov. 2018, doi: 10.1109/JSEN.2018.2868340.
- [25] R. A. Romeo, C. M. Oddo, M. C. Carrozza, E. Guglielmelli, and L. Zollo, "Slippage Detection with Piezoresistive Tactile Sensors," *Sensors*, vol. 17, no. 8, p. 1844, Aug. 2017, doi: 10.3390/s17081844.
- [26] W. R. Provancher and N. D. Sylvester, "Fingerpad Skin Stretch Increases the Perception of Virtual Friction," *IEEE Trans. Haptics*, vol. 2, no. 4, pp. 212–223, Oct. 2009, doi: 10.1109/TOH.2009.34.
- [27] Z. F. Quek, S. B. Schorr, I. Nisky, A. M. Okamura, and W. R. Provancher, "Sensory augmentation of stiffness using fingerpad skin stretch," in 2013 World Haptics Conference (WHC), Apr. 2013, pp. 467–472. doi: 10.1109/WHC.2013.6548453.
- [28] Y. Wang, K. L. Marshall, Y. Baba, E. A. Lumpkin, and G. J. Gerling, "Compressive Viscoelasticity of Freshly Excised Mouse Skin Is Dependent on Specimen Thickness, Strain Level and Rate," *PLOS ONE*, vol. 10, no. 3, p. e0120897, Mar. 2015, doi: 10.1371/journal.pone.0120897.
- [29] R. LaMotte and M. Srinivasan, "Tactile discrimination of shape: responses of rapidly adapting mechanoreceptive afferents to a step stroked across the monkey fingerpad," *J. Neurosci.*, vol. 7, no. 6, pp. 1672–1681, Jun. 1987, doi: 10.1523/JNEUROSCI.07-06-01672.1987.
- [30] D. A. Poulos et al., "The Neural Signal for the Intensity of a Tactile Stimulus," J. Neurosci., vol. 4, no. 8, pp. 2016–2024, 1984.
- [31] S. Simonetti, K. Dahl, and C. Krarup, "Different indentation velocities activate different populations of mechanoreceptors in humans," *Muscle Nerve*, vol. 21, no. 7, pp. 858–868, 1998, doi: 10.1002/(SICI)1097-4598(199807)21:7<858::AID-MUS3>3.0.CO;2-5.
- [32] S. C. Hauser and G. J. Gerling, "Imaging the 3-D deformation of the finger pad when interacting with compliant materials," in *IEEE Haptics Symposium, HAPTICS*, May 2018, vol. 2018-March, pp. 7–13. doi: 10.1109/HAPTICS.2018.8357145.

- [33] B. Li, S. Hauser, and G. J. Gerling, "Identifying 3-D spatiotemporal skin deformation cues evoked in interacting with compliant elastic surfaces," in 2020 IEEE Haptics Symposium (HAPTICS), Mar. 2020, pp. 35–40. doi: 10.1109/HAPTICS45997.2020.ras.HAP20.22.5a9b38d8.
- [34] E. Miguel et al., "Characterization of nonlinear finger pad mechanics for tactile rendering," in *IEEE World Haptics Conference*, WHC 2015, 2015. doi: 10.1109/WHC.2015.7177692.
- [35] G. J. Gerling, S. C. Hauser, B. R. Soltis, A. K. Bowen, K. D. Fanta, and Y. Wang, "A Standard Methodology to Characterize the Intrinsic Material Properties of Compliant Test Stimuli," *IEEE Trans. Haptics*, vol. 11, no. 4, pp. 498–508, Oct. 2018, doi: 10.1109/TOH.2018.2825396.
- [36] S. C. Hauser and G. J. Gerling, "Measuring tactile cues at the fingerpad for object compliances harder and softer than the skin," in 2016 IEEE Haptics Symposium (HAPTICS), Apr. 2016, pp. 247–252. doi: 10.1109/HAPTICS.2016.7463185.
- [37] C. Xu and G. J. Gerling, "Time-dependent Cues Encode the Minimum Exploration Time in Discriminating Naturalistic Compliances," in 2020 IEEE Haptics Symposium (HAPTICS), Mar. 2020, pp. 22–27. doi: 10.1109/HAPTICS45997.2020.ras.HAP20.7.ec43f6a7.
- [38] A. Metzger and K. Drewing, "Effects of Stimulus Exploration Length and Time on the Integration of Information in Haptic Softness Discrimination," *IEEE Trans. Haptics*, vol. 12, no. 4, pp. 451–460, Oct. 2019, doi: 10.1109/TOH.2019.2899298.
- [39] A. Metzger, A. Lezkan, and K. Drewing, "Integration of serial sensory information in haptic perception of softness," *J. Exp. Psychol. Hum. Percept. Perform.*, vol. 44, no. 4, pp. 551–565, 2018, doi: 10.1037/xhp0000466.
- [40] H. Z. Tan, N. I. Durlach, G. L. Beauregard, and M. A. Srinivasan, "Manual discrimination of compliance using active pinch grasp: the roles of force and work cues," *Percept. Psychophys.*, vol. 57, no. 4, pp. 495–510, May 1995, doi: 10.3758/bf03213075.
- [41] L. Kaim and K. Drewing, "Exploratory Strategies in Haptic Softness Discrimination Are Tuned to Achieve High Levels of Task Performance," *IEEE Trans. Haptics*, vol. 4, no. 4, pp. 242–252, Oct. 2011, doi: 10.1109/TOH.2011.19.
- [42] L. Willemet, K. Kanzari, J. Monnoyer, I. Birznieks, and M. Wiertlewski, "Initial contact shapes the perception of friction," *Proc. Natl. Acad. Sci.*, vol. 118, no. 49, p. e2109109118, Dec. 2021, doi: 10.1073/pnas.2109109118.
- [43] B. M. Dzidek, M. J. Adams, J. W. Andrews, Z. Zhang, and S. A. Johnson, "Contact mechanics of the human finger pad under compressive loads," *J. R. Soc. Interface*, vol. 14, no. 127, p. 20160935, Feb. 2017, doi: 10.1098/rsif.2016.0935.
- [44] M. Tomimoto, "The frictional pattern of tactile sensations in anthropomorphic fingertip," *Tribol. Int.*, vol. 44, no. 11, pp. 1340–1347, Oct. 2011, doi: 10.1016/j.triboint.2010.12.004.
- [45] T. Maeno, K. Kobayashi, and N. Yamazaki, "Relationship between the Structure of Human Finger Tissue and the Location of Tactile Receptors," *JSME Int. J. Ser. C*, vol. 41, no. 1, pp. 94–100, 1998, doi: 10.1299/jsmec.41.94.



Bingxu Li received the BA degree in Industrial and Enterprise Systems Engineering from the University of Illinois at Urbana-Champaign and MS degree in Systems Engineering from the University of Virginia, in 2018 and 2020, respectively. She is currently working toward the PhD degree. The focus of her research is

on haptics, compliance perception, biomechanics, human-computer interaction, tactile sensors and actuators.



Steven C. Hauser received the BA degree in Computer Science, the MS degree in Biomedical Engineering, and the PhD degree in Systems Engineering from the University of Virginia, in 2014, 2016, and 2019, respectively. The focus of his research is on haptics, compliance perception, and psychophysics.



Gregory J. Gerling received the PhD degree from the Department of Mechanical and Industrial Engineering at the University of Iowa in 2005. Currently, he is a professor in Systems Engineering at the University of Virginia, with appointments in Mechanical and Biomedical Engineering. He has served as co-chair of the IEEE

Haptics Symposium, associate editor-in-chief of the IEEE World Haptics Conference, and is currently chair of the IEEE Technical Committee on Haptics and associate editor of the IEEE Transactions on Haptics. His research interests include haptics, computational neuroscience, biomechanics, and human-computer interaction.